

# How social network influences human behavior: An integrated latent space approach

Ick Hoon Jin\*, Jina Park, and Minjeong Jeon

September 14, 2021

## Abstract

How human behavior is influenced by a social network that they belong has been an interested topic in applied research. Existing methods often utilized scale-level behavioral data to estimate the influence of a social network on human behavior. This study proposes a novel approach to studying social influence by using item-level behavioral measures. Under the latent space modeling framework, we integrate the two latent spaces for respondents' social network data and item-level behavior measures. We then measure social influence as the impact of the latent space configuration contributed by the social network data on the behavior data. The performance and properties of the proposed approach are evaluated via simulation studies. We apply the proposed model to an empirical dataset to explain how students' friendship network influences their participation in school activities.

**Keywords:** Social influence; Network analysis; Item response model; Latent space model; Latent space item response model; Peer Network

---

\*Ick Hoon Jin and Jina Park, Department of Applied Statistics, Department of Statistics and Data Science, Yonsei University; Minjeong Jeon, School of Education and Information Studies, University of California, Los Angeles. This study was partially supported by the Yonsei University Research Fund 2019-22-0210 and by Basic Science Research Program through the National Research Foundation of Korea (NRF 2020R1A2C1A01009881). Correspondence should be addressed to Ick Hoon Jin, Department of Applied Statistics, Department of Statistics and Data Science, Yonsei University, Seoul, Republic of Korea. E-Mail: [ijin@yonsei.ac.kr](mailto:ijin@yonsei.ac.kr). Jin and Park are co-first authors.

# 1 Introduction

A frequently asked question in education and social science research is how contexts influence the behavioral outcomes of individuals. The influence process can take various forms. For example, emotional or social support networks that students have in classrooms with their teachers, mentors, or friends are likely to play an important role in that process. The impact of individuals' social networks on their behavior is often referred to as *social influence* in the literature (Sun and Tang, 2011; Sijtsema et al., 2010; Simpkins et al., 2013; Shakarian et al., 2015).

Social influence has widely been studied in applied research using various analytic methods for both cross-sectional and longitudinal data. For instance, Urberg et al. (1997) and Mercken et al. (2010) investigated how a network of close friends influenced adolescents' smoking behavior with cross-sectional and longitudinal analysis, respectively. Cheng et al. (2014) analyzed cross-sectional data on high school adolescents to examine how friends' physical activities were influenced the adolescents' physical activity levels. Vitale et al. (2016) examined how students' academic performance was influenced by their shared interest network by applying a longitudinal network analysis.

In this study, we propose a new statistical modeling approach to identifying social influence effects in the cross-sectional network and item-level behavior data. The key observation behind our idea is that in the social influence literature, behaviors of interest are processed at the scale level and treated as a person (actor)-level variable for analysis (Ord, 1975; Doreian, 1989; Leenders, 2002; Dittrich et al., 2019; Robins et al., 2001; Daraganova and Robins, 2013; Sweet and Adhikari, 2020). However, the human mind and behaviors, such as cognitive and non-cognitive abilities, psychology, and attitudes, are latent variables, typically measured based on multiple items. Here we propose to model the behaviors of interest with the item-level data in the proposed approach. By doing so, we essentially have two statistical models for individuals' item-level behavior data and social network data; then, the task of examining social influences comes down to integrating the two statistical models.

We will model the two types of data in a common modeling framework based on latent spaces: the latent space model (LSM) for social network data (Hoff et al., 2002) and the latent space item response model (LSIRM; Jeon et al. 2021) for item response behavior data. The LSM, a widely used approach to social network data, measures the distances between the latent positions of individuals to model the probabilities of ties among them. The between-people distances indicate individuals' interactions in the network of interest, where shorter distances indicate stronger between-people connections. The LSIRM, a recent development in the psychometrics literature, is a specialized extension of the LSM in item

response analysis. The LSIRM views binary item response data as bipartite network data that represent relationships between respondents and items. It measures the distances between respondents and items as a penalty term to model the respondents' probabilities of giving correct (or positive) responses, where the respondent-item distances represent their relations given the respective main effects. Shorter respondent-item distances, for example, indicate the respondents have stronger relations with the items, meaning that the respondents are likely to provide positive responses to those items.

A common feature of the LSM and the LSIRM is that both models locate individuals in a latent space based on their relationships with peers (for the social network) and with behavior items (for the item response network). Based on the two latent spaces of individuals, we postulate that social influence can be understood by evaluating how the latent positions of individuals in the social network (i.e., their social relationships) impact their latent positions in the behavior response network (i.e., their relationships with behavior measured with the items). With this assumption, we set up the latent space for behavior response data with individuals' latent positions from their social network space. Then the locations of individual respondents in the behavior response network reflect the individuals' social relationships with their peers. The adapted latent space tells us how respondents in social groups responded to the behavior items of interest, helping us overview the structure and patterns of social influence. We can also measure the size and direction of overall social influence by estimating the impact of the adapted latent space on behavior response data after controlling for the target trait levels of individuals and the difficulty levels of behavior items.

We applied the proposed method to an empirical dataset to examine how students' friendship with peers (social network) influence their participation in school activities (behavior). We developed a fully Bayesian method to estimate the proposed joint models and conducted simulation studies to evaluate and support the performance of the proposed approach.

The rest of the paper is organized as follows. In Section 2, we started by providing some background of the proposed approach. We briefly described the latent space modeling framework for social network data (LSM) and item response data (LSIRM). We also discussed some existing social influence models in the literature. In Section 3, we presented the formulation of the proposed Bayesian model for social influence. We provided details of the Bayesian estimation procedure. In Section 4, we provided a real data example with a detailed analysis of the proposed approach. In Section 5, we presented our simulation studies to evaluate the performance of our proposed approach. Finally, we concluded our paper with a summary and discussion in Section 6.

## 2 Background

### 2.1 Latent Space Model

The latent space model (Hoff et al. 2002; Handcock et al. 2007; Krivitsky et al. 2009; Raftery et al. 2012; Rastelli et al. 2016; Sewell and Chen 2015; Gollini and Murphy 2016) is one of the well-developed statistical models for analyzing network data. In LSM, the probability of an edge between node  $k$  and  $l$  depends on the distance between their latent positions in a  $D$ -dimensional Euclidean latent space. In general, the smaller the distance between nodes in the latent space, the greater the probability they are connected.

To formulate the model, let  $\mathbf{Y}_{n \times n}$  be a peer network among respondents where  $y_{kl}$  is a connection between respondent  $k$  and  $l$ . Note that  $\mathbf{Y}$  is an undirected network and there are no self-edges in network  $\mathbf{Y}$ . Let  $\mathbf{Z}$  be a  $N \times D$  latent position matrix where  $\mathbf{z}_k = (z_{k1}, \dots, z_{kD})$  is the  $D$ -dimensional vector indicating the position of node  $k$  in the  $D$ -dimensional latent space. Let  $\alpha$  be the intercept term of LSM and  $\gamma$  be the weight parameter of the Euclidean distance term. Let  $\Theta^n = \{\mathbf{Z}, \alpha, \gamma\}$  be the collection of model parameters of the LSM, where superscript  $n$  represents that the parameter set for the LSM. Then, LSM can then be written as

$$P(\mathbf{Y} \mid \Theta^n) = \prod_{k \neq l} P(y_{kl} \mid \mathbf{z}_k, \mathbf{z}_l, \alpha, \gamma) = \prod_{k \neq l} \frac{\exp(\alpha - \gamma \|\mathbf{z}_k - \mathbf{z}_l\|)^{y_{kl}}}{1 + \exp(\alpha - \gamma \|\mathbf{z}_k - \mathbf{z}_l\|)}, \quad (1)$$

where  $\|\mathbf{z}_k - \mathbf{z}_l\|$  is the Euclidean distance between node  $k$  and  $l$  in a low-dimensional Euclidean space. We selected a two-dimensional space in this paper, which has convenience for visualization and is a conventional choice in the literature. The weight parameter  $\gamma \geq 0$  for the distance term represents the magnitude of social interactions present in the network data of interest. Weight  $\gamma$  is assumed to be positive, so that a larger distance indicates weaker connections between people.  $\gamma = 0$  indicates no meaningful presence of social interactions in the peer network data. The LSM with  $\gamma = 0$  is equivalent to the Erdős-Renyi model (Erdős and Rényi, 1960), in which each edge is independent of the connections of other pairs and connection probability for all nodes is same.

To estimate the LSM model parameters, a Bayesian approach is frequently used (Berlusconi et al., 2017; Salter-Townshend and McCormick, 2017; Sewell and Chen, 2017; Liu et al., 2020). The prior distributions for the model parameters can be given as

$$\alpha \sim N(0, \sigma_\alpha^2), \quad \mathbf{z}_k \sim N(\mathbf{0}, \mathbf{I}_d), \quad \text{and} \quad \log(\gamma) \sim N(0, \sigma_\gamma^2). \quad (2)$$

Here we assume that  $\mathbf{z}_k$  follows an independent spherical multivariate normal distribution. To estimate the weight parameter  $\gamma$ , we fix the scale of the  $\mathbf{z}_k$  to one.

Distances between respondents, i.e., their relationship with others can be represented in a two-dimensional Euclidean space as illustrated in Figure 1(a). The latent space shown in Figure 1(a) represents a close friend network of 539 US middle school students, while small light blue dots represent the students. Shorter distances between dots indicate closer relationships or a higher likelihood of their being close friends. This latent space shows that there are roughly four groups or sub-networks of close friends in this chosen school (this is School 59 from the empirical example described in Section 4).

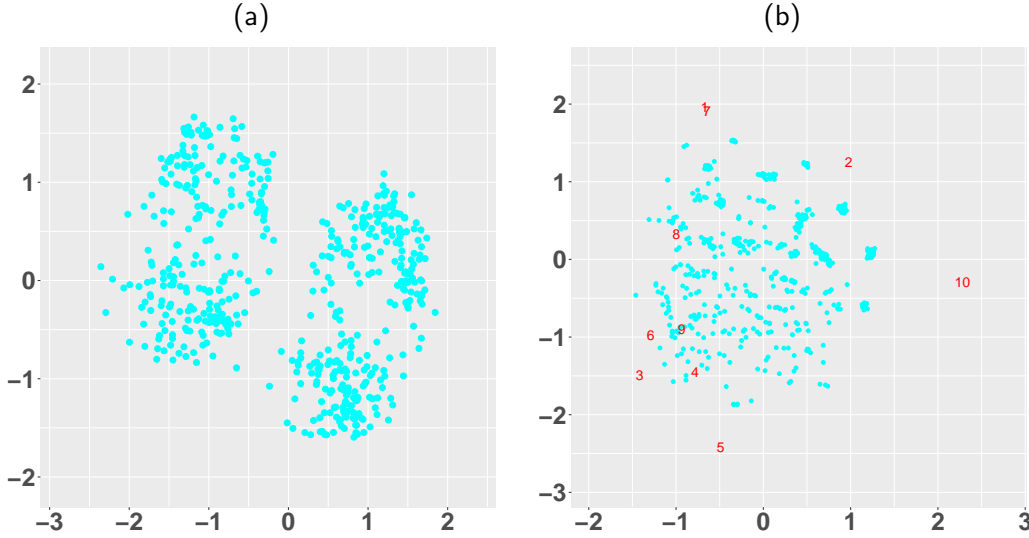


Figure 1: (a) A latent space of close friends of 539 US middle school students estimated based on the LSM. Blue dots represent students. (b) A latent space of students and test items is estimated based on the LSIRM. Red numbers represent ten school activity items, and colored dots represent students.

## 2.2 Latent Space Item Response Model

A latent space item response model (LSIRM; Jeon et al., 2021) is a unique extension of LSM for binary item response data. LSIRM assumes both item and respondents are embedded in a low-dimensional latent space, such that the probability of a correct (or positive) response decreases by the distance between the respondents' and the items' position in the latent space. The resulting latent space represents the interactions between respondents and items, after taking into account the person and item characteristics (e.g., person ability and item difficulty) as main effects.

To formulate the LSIRM, suppose  $\mathbf{X}_{n \times p}$  is an item response dataset where  $x_{ki}$  is a binary response of respondent  $k$  to item  $i$ . Let  $\beta = \{\beta_i\}$  and  $\theta = \{\theta_k\}$  be the item easiness parameter and person characteristic parameter, respectively. Let  $\mathbf{Z}$  and  $\mathbf{W}$  be a  $N \times D$  and  $P \times D$  latent position matrix

where  $\mathbf{z}_k = (z_{k1}, \dots, z_{kD})$  and  $(w_{i1}, \dots, w_{iD})$  are the  $D$ -dimensional vector indicating the position of respondent  $k$  and that indicating the position of item  $i$ , respectively. Let  $\Theta^r = \{\beta, \theta, \mathbf{Z}, \mathbf{W}, \delta, \sigma^2\}$  be the collection of the LSIRM model parameters, where superscript  $r$  represents the parameter set for the LSIRM. Then, LSIRM can be written as

$$P(\mathbf{X} | \Theta^r) = \prod_{k=1}^n \prod_{i=1}^p P(x_{ki} | \beta_i, \theta_k, \gamma, \mathbf{z}_k, \mathbf{w}_i) = \prod_{k=1}^n \prod_{i=1}^p \frac{\exp(\beta_i + \theta_k - \gamma \|\mathbf{z}_k - \mathbf{w}_i\|)^{x_{ki}}}{1 + \exp(\beta_i + \theta_k - \gamma \|\mathbf{z}_k - \mathbf{w}_i\|)}, \quad (3)$$

where  $\|\mathbf{z}_k - \mathbf{w}_i\|$  is the Euclidean distance between the latent positions of respondent  $k$  and item  $i$  and  $\gamma > 0$  is the weight of the distance term. As in the LSM, we chose a two-dimensional Euclidean space to represent respondent-item distances from the LSIRM.  $\gamma > 0$  ensures that a large respondent-item distance decreases the probability of the respondent's giving a correct (or positive) response to the item. Further, the weight parameter  $\gamma$  is of crucial importance as it represents the importance or impact of the latent space (of respondents and items) on the success probability of giving positive responses, after taking into account the person and item main effects,  $\theta_k$  and  $\beta_i$ . When  $\gamma = 0$ , the LSIRM reduces to a conventional item response model, specifically the Rasch model, which assumes the main effects,  $\theta_k$  and  $\beta_i$  are sufficient to explain the the success probability.

A Bayesian approach is used to estimate the LSIRM. Prior distributions of the LSIRM parameters can be given as follows:

$$\begin{aligned} \beta_i &\sim \mathcal{N}(0, \sigma_\beta^2), \quad \theta_k | \sigma^2 \sim \mathcal{N}(0, \sigma^2), \quad \sigma^2 \sim \text{Inv-G}(a_\sigma, b_\sigma), \\ \mathbf{w}_i &\sim \mathcal{N}(\mathbf{0}, \mathbf{I}_d), \quad \mathbf{z}_i \sim \mathcal{N}(\mathbf{0}, \mathbf{I}_d), \quad \text{and} \quad \log(\gamma) \sim \mathcal{N}(0, \sigma_\gamma^2). \end{aligned} \quad (4)$$

Figure 1(b) illustrates an estimated two-dimensional latent space from the LSIRM. Blue dots represent the 539 US middle school students, the same students used in Figure 1(a), while red numbers represent ten items about students' school activities. Details of the data and items are described in Section 4. Shorter distances between respondents and test items indicate that the respondents were more likely to respond positively to the items (i.e., they had a higher probability of participating in the corresponding school activities). It is important to mention that respondents in a similar region tend to show a similar profile of the measured behaviors. For example, respondents on the bottom left of the space are pretty close to Items 3, 4, 6, and 9, while far apart from items 2 and 10. This means that those respondents are similar in terms of their school activity patterns, such that they are more likely to participate in activities 3, 4, 6, and 9 but less likely to participate in the school activity of 2 (sports outside school) and 10 (video games) given their overall activity levels.

### 2.3 Existing Social Influence Models

Network autocorrelation models are a widely-used method to study social influence with longitudinal data (Ord, 1975; Doreian, 1989; Leenders, 2002; Dittrich et al., 2019). These models quantify the strength of a peer effect on a network (e.g., social influence) while controlling for individuals' characteristics and network autocorrelations (Frank et al., 2004; Zheng et al., 2010; Scott et al., 2012; Fujimoto et al., 2013). Suppose  $\mathbf{y}$  is a vector containing measures on a response variable. A linear network autocorrelation model can be given as follows:

$$\mathbf{y} = \rho W \mathbf{y} + \epsilon, \quad (5)$$

where  $\rho$  is a network autocorrelation parameter, and  $W = \{w_{ij}\}$  is a matrix of influence coefficients that indicate the influence of actor  $j$  on actor  $i$ ; the error term  $\epsilon \sim N(0, \sigma^2 I)$  (Leenders, 2002). This model is extended by including covariates  $X$ :

$$\mathbf{y} = \rho W \mathbf{y} + X\beta + \epsilon, \quad (6)$$

where  $\epsilon \sim N(0, \sigma^2 I)$ . This extended model is also referred to as the regressive- autoregressive model Ord (1975) or the network effects model Doreian (1989). Other extensions models are also available (e.g., Ord, 1975; Doreian, 1980; Dow et al., 1982; Doreian, 1982; Doreian, 1989; Rietveld and Wintershoven, 1998).

A related model is the autologistic actor attribute model (ALAAM; Robins et al. 2001; Daraganova and Robins 2013). This model leverages exponential random graph models (ERGM; Fienberg 2012; Robins et al. 2007; Hunter 2007) for network configuration. The autologistic actor attribute model specifies the probability of observing attributes (behaviors)  $\mathbf{y}$  given network  $\mathbf{x}$  (Parker et al., 2021):

$$P(\mathbf{y}|\mathbf{x}) = \frac{1}{\kappa(\boldsymbol{\theta})} \exp \left( \sum_{i=1}^p \theta_i s_i(\mathbf{y}, \mathbf{x}, \mathbf{w}) \right),$$

where  $s_i(\mathbf{y}, \mathbf{x}, \mathbf{w})$  is a network statistic that involves interactions among attributes  $\mathbf{y}$ , network data  $\mathbf{x}$ , and other actor-specific characteristics  $\mathbf{w}$ ,  $\theta_i$  is the corresponding parameter for  $s_i(\mathbf{y}, \mathbf{x}, \mathbf{w})$ , and  $\kappa(\boldsymbol{\theta})$  is a normalizing constant to ensure the proper probability distribution. The autologistic actor attribute model can be applied to the cross-sectional network data.

In addition, latent space modeling (LSMs) approaches introduced in Section 2.1 have also been used to study social influence. For example, Sweet and Adhikari (2020) recently proposed how latent space modeling for network data can be used in the autocorrelation model presented in Equations (5) and

(6). Specifically, they proposed replacing the weight matrix  $W$  of the network autocorrelation model (5) and (6) with the affinity matrix calculated from the latent positions of people estimated based on the LSM. This model can also be applied to cross-sectional data. The model explained above is related to our proposed model because both utilize latent space modeling approaches for identifying social relationships between respondents from the network data of interest. However, the two models are different in terms of how respondents' social relationships are used for understanding and estimating their impacts on the respondents' behavioral outcomes. The model above is based on the auto-correlation model for behaviors, whereas our approach is based on the latent space model for behavior data. In the subsequent section, we elaborate on how the proposed model is formulated to estimate social influence in an integrated latent space modeling framework.

### 3 Model

In the proposed framework for social influence, we measure whether and how an individual's behaviors, i.e., their responses to behavior items, are influenced by the peer network to which the individuals belong. If social influence plays a role, individuals with stronger connections in the peer network are likely to show a higher level of similarity in their behavior. In the latent space framework, this means that those who are closer in the latent space of social networks are likely to show similar distances to behavior items (i.e., similar profiles of behaviors) in the latent space for behavior item response data.

We propose adopting the LSIRM for behavior item response data to estimate social influence in this framework by integrating it with the LSM for social network data. We call the adapted model the *LSIRM for social influence*. The framework of the LSIRM for social influence is represented in Figure 2.

As shown in Figure 2, two types of datasets are required to apply the proposed approach:  $\mathbf{X}_{n \times p}$  for an item response matrix and  $\mathbf{Y}_{n \times n}$  for a peer network matrix, where  $n$  is the number of respondents, and  $p$  is the number of items (from the test used to measure the target behavior of interest). Subscripts of  $\mathbf{X}$  and  $\mathbf{Y}$  are suppressed from now on for succinctness.

#### 3.1 LSIRM for Social Influence

To estimate social influence effects  $\delta$  in Figure 2, we propose the following two-step estimation approach: (1) First, estimate the parameters of the LSM with the social network data  $Y$  (Equation (1)) and obtain the estimated respondent latent position matrix  $\hat{\mathbf{Z}}$ ; (2) Second, estimate the adapted LSIRM by fixing the latent positions of respondents to  $\hat{\mathbf{Z}}$  from the LSM, where  $\delta$  now represents the impact of the



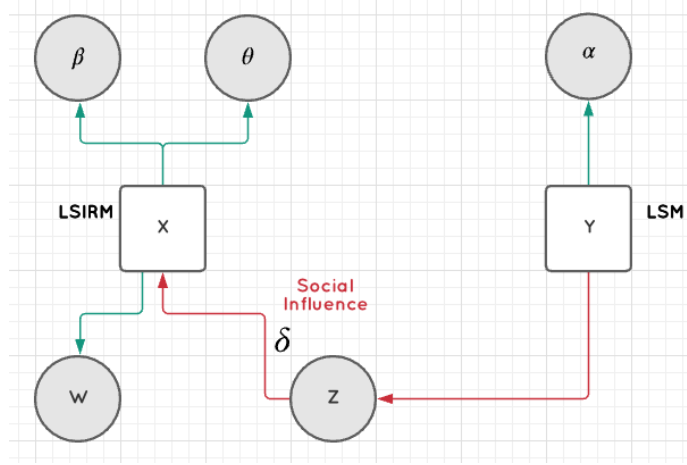


Figure 2: LSIRM for social influence. This diagram shows how social influence can be estimated with the revised LSIRM (for behavior response data  $X$ ) connected to the LSM (for social network  $Y$ ). The red line with an arrowhead shows the process of social influence. Social influence is estimated as the impact of the individuals' relationship structure ( $Z$ ) obtained from network data  $Y$  through the LSM on the item-level behavior response data  $X$ .

updated latent space of respondents and items on the behavior response data.

If social influence exists, the positions of behavior items in the adapted LSIRM are determined such that individuals who have stronger connections in the peer network have similar distances to the behavior items. Therefore, the impact of the estimated latent space configuration from the adapted LSIRM, represented by the  $\delta$  parameter, can tell us the presence and degree of overall social influence in the data. The adapted LSIRM for social influence can be formulated as follows:

$$P(\mathbf{X} | \hat{\mathbf{Z}}, \Theta^{r*}) = \prod_{k=1}^n \prod_{i=1}^p \frac{\exp(\beta_i + \theta_k - \delta \|\hat{\mathbf{z}}_k - \mathbf{w}_i\|)}{1 + \exp(\beta_i + \theta_k - \delta \|\hat{\mathbf{z}}_k - \mathbf{w}_i\|)}^{x_{ki}}, \quad (7)$$

where  $\Theta^{r*} = \{\beta, \theta, \mathbf{W}, \delta, \sigma^2\}$  is the collection of the adapted LSIRM model parameters and  $\hat{\mathbf{Z}}$  is the matrix of respondent distances estimated from the LSM, representing the respondents' social relationships.

As shown above, the adapted LSIRM in Equation (7) assumes the latent positions of individuals are known; they represent the individuals' relationships with others (estimated based on peer network data with the LSM). In that sense, the adapted LSIRM is different from the standard LSIRM in Equation (3), where individuals' latent positions are the parameters to be estimated and represent their relationships to behavior items. Because the latent space represented in Equation (7) is not the same as the latent

space represented in Equation (3), we use  $\delta$  in Equation (7) to quantify the impact of the adapted latent space on the success probability of item-level behavior data.

**Configuration of adapted latent space** The positions of behavior items and their distances to respondents obtained from the LSIRM help us understand how people with stronger or weaker social connections have responded to the behavior items. Because the positions of individuals have been determined based on their peer network ( $\hat{\mathbf{Z}}$ ), respondents with stronger social connections are closer to each other than others with weaker social connections in the latent space obtained from the adapted LSIRM. For example, suppose two respondents, A and B were close to each other in an estimated adapted latent space. Also, three behavior items 1, 2, and 3 were close to respondents A and B. This means that the two respondents with stronger social connections had a similar likelihood of showing the three types of behaviors measured by the three items). In this sense, the configuration of the latent space from the adapted LSIRM reflects the structure or patterns of social influence.

**More on the weight parameter  $\delta$**  Because the latent space configuration from the adapted latent space reflects the pattern of social influence, the weight parameters  $\delta$  that quantifies the impact or importance of the latent space on behavior data can be seen as average or overall social influence effects in the data. For example,  $\delta = 0$  indicates that respondents' connections to their peers rarely affect or explain their behavior.

It is worth mentioning that  $\delta$  can be either positive or negative in the adapted LSIRM. This is an additional difference from the standard LSIRM that assumes  $\gamma \geq 0$ . In the adapted LSIRM for social influence, we assume  $\delta \in \mathbb{R}$  because the sign of  $\delta$  indicates the overall direction of social influence effects in the data. For example, suppose two close respondents in the adapted latent space were far away from a behavior item. The two individuals being close to each other in the space means that they had stronger social connections. In this setting,  $\delta > 0$  indicates that the two people were less likely to show the behavior (measured by the item), whereas  $\delta < 0$  means that they were more likely to display the behavior. That is,  $\delta > 0$  a large distance to items decreases the likelihood of endorsing the items, whereas with  $\delta < 0$  a large distance to items increases the likelihood of endorsing the items (i.e., likelihood of showing the behaviors represented by the items).

**Example** Figure 3 illustrates a latent space estimated based on the adapted LSIRM for social influence. The same dataset used in Figure 1(a) and (b); red numbers are ten school activity items, and colored dots are US middle school students. Student locations and their distances to others represent their close

friend network, and the configuration is the same as shown in Figure 1(a) from the LSM for the social network data. The item locations and their configurations are somewhat different from the patterns that we see in Figure 1(b) from the standard LSIRM for the school activity item response data because, in this adapted space, the item configuration reflects the shared response patterns of close friends of the middle school students. For example, students in purple in the adapted latent space (located in the east region of the space) are particularly close to school activities 1 (sports) and 7 (dating) but further away from activity 10 (video games), meaning that the students in the corresponding close friend group showed a similar pattern of school activities.

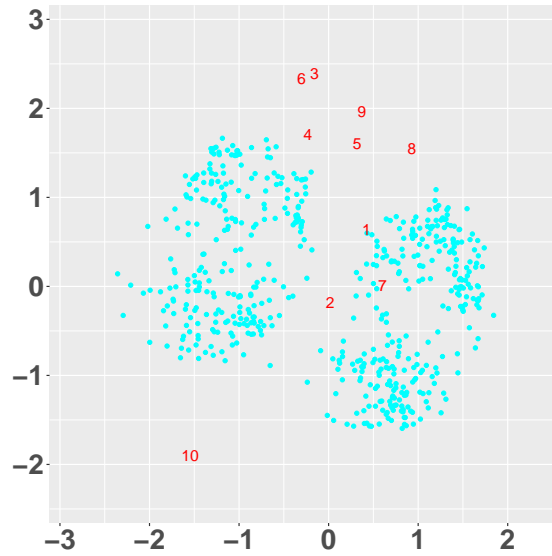


Figure 3: An illustration of an adapted latent space for social influence. Red numbers represent ten school activity items, and colored dots represent 539 US middle school students (same as the data used in Figure 1(a) and (b)).

### 3.2 MCMC Implementation

We apply a fully Bayesian method for estimating the proposed approach using Markov chain Monte Carlo (MCMC). We apply a two-step estimation approach to estimate the proposed adapted LSIRM for social influence, where, in step 1, we estimate the standard LSM for social network data, and, in step 2, we estimate the adapted LSIRM by fixing respondent latent positions to the estimated respondent positions from Step 2. MCMC sampling at each step is detailed below.

**Step 1: Estimation of the LSM** The posterior distribution of the Bayesian LSM for social network data can be written as follows:

$$\begin{aligned}\pi(\Theta^n | \mathbf{Y}) &\propto P(\mathbf{Y} | \Theta^n) \pi(\alpha) \pi(\gamma) \pi(\mathbf{Z}) \\ &= \prod_{k \neq l} \frac{\exp(\alpha - \gamma \|\mathbf{z}_k - \mathbf{z}_l\|)^{y_{kl}}}{1 + \exp(\alpha - \gamma \|\mathbf{z}_k - \mathbf{z}_l\|)} \pi(\alpha) \pi(\gamma) \pi(\mathbf{Z}),\end{aligned}\quad (8)$$

where  $\mathbf{Y}$  is  $n \times n$  social network data for  $n$  respondents,  $\Theta^n = \{\mathbf{Z}, \alpha, \gamma\}$  is the parameter space of the LSM, and  $P(\mathbf{Y} | \Theta^n)$  is the LSM for social network data  $\mathbf{Y}$ , which was given in Equation (1). Prior distributions  $\pi(\alpha)$ ,  $\pi(\gamma)$ , and  $\pi(\mathbf{Z})$  were provided in Equation (2). The sampling process from the posterior can be given as follows at  $t$ :

**1. Update the latent position of respondents.**

For  $k = 1, \dots, n$ ,

$$r(\mathbf{z}_k^*, \mathbf{z}_k^{(t)}) = \frac{\pi(\mathbf{z}_k^*)}{\pi(\mathbf{z}_k^{(t)})} \frac{P(\mathbf{Y} | \mathbf{z}_k^*, \mathbf{Z}_{-k}, \Theta_{-\mathbf{Z}}^n)}{P(\mathbf{Y} | \mathbf{z}_k^{(t)}, \mathbf{Z}_{-k}, \Theta_{-\mathbf{Z}}^n)} \frac{q(\mathbf{z}_k^* \rightarrow \mathbf{z}_k^{(t)})}{q(\mathbf{z}_k^{(t)} \rightarrow \mathbf{z}_k^*)},$$

where  $\mathbf{Z}_{-k} = (\mathbf{z}_1, \dots, \mathbf{z}_{k-1}, \mathbf{z}_{k+1}, \dots, \mathbf{z}_n)$  and  $\Theta_{-\mathbf{Z}}^n$  is the parameter sets for LSM except  $\mathbf{Z}$ , respectively.

**2. Update the intercept parameter,  $\alpha$ , of LSM.**

$$r(\alpha^*, \alpha^{(t)}) = \frac{\pi(\alpha^*)}{\pi(\alpha^{(t)})} \frac{P(\mathbf{Y} | \alpha^*, \Theta_{-\alpha}^n)}{P(\mathbf{Y} | \alpha^{(t)}, \Theta_{-\alpha}^n)} \frac{q(\alpha^* \rightarrow \alpha^{(t)})}{q(\alpha^{(t)} \rightarrow \alpha^*)}.$$

where  $\Theta_{-\alpha}^n$  is the parameter set for LSM except  $\alpha$ .

**3. Update the weight parameter of the distance term,  $\gamma$ .**

$$r(\gamma^*, \gamma^{(t)}) = \frac{\pi(\gamma^*)}{\pi(\gamma^{(t)})} \frac{P(\mathbf{Y} | \gamma^*, \Theta_{-\gamma}^n)}{P(\mathbf{Y} | \gamma^{(t)}, \Theta_{-\gamma}^n)} \frac{q(\gamma^* \rightarrow \gamma^{(t)})}{q(\gamma^{(t)} \rightarrow \gamma^*)}$$

where  $\Theta_{-\gamma}^n$  is the parameter set for LSM except  $\gamma$ .

**Step 2: Estimation of the adapted LSIRM for social influence** The posterior distribution of the adapted LSIRM for social influence can be written as follows:

$$\begin{aligned}\pi(\Theta^{r*} | \mathbf{X}, \hat{\mathbf{Z}}) &\propto P(\mathbf{X} | \hat{\mathbf{Z}}, \Theta^{r*}) \pi(\beta) \pi(\theta | \sigma^2) \pi(\sigma^2) \pi(\mathbf{W}) \pi(\delta) \\ &= \prod_{k=1}^n \prod_{i=1}^p \frac{\exp(\beta_i + \theta_k - \delta \|\hat{\mathbf{z}}_k - \mathbf{w}_i\|)^{x_{ki}}}{1 + \exp(\beta_i + \theta_k - \delta \|\hat{\mathbf{z}}_k - \mathbf{w}_i\|)} \pi(\beta) \pi(\theta | \sigma^2) \pi(\sigma^2) \pi(\mathbf{W}) \pi(\delta),\end{aligned}\quad (9)$$

where  $\mathbf{X}$  is the  $n \times p$  item response data for  $n$  respondents to  $p$  behavior items,  $\Theta^{r*} = \{\beta, \theta, \mathbf{W}, \delta, \sigma^2\}$  is the parameter space for the adapted LSIRM,  $P(\mathbf{X} | \hat{\mathbf{Z}}, \Theta^{r*})$  is the adapted LSIRM given  $\hat{\mathbf{Z}}$ , the respondent latent positions obtained from Step 1. Prior distributions for  $\beta_i$ ,  $\theta_k$ ,  $\sigma^2$ , and  $\mathbf{w}_i$  were given in (4). For  $\delta$ , we assign  $\delta \sim \mathcal{N}(0, \sigma_\delta^2)$ . The sampling process from the posterior is given below at  $t$ :

**1. Update the latent position of items.**

For  $i = 1, \dots, p$ ,

$$r(\mathbf{w}_i^*, \mathbf{w}_i^{(t)}) = \frac{\pi(\mathbf{w}_i^*)}{\pi(\mathbf{w}_i^{(t)})} \frac{P(\mathbf{X} | \mathbf{w}_i^*, \mathbf{W}_{-i}, \Theta_{-\mathbf{W}}^{r*}, \hat{\mathbf{Z}})}{P(\mathbf{X} | \mathbf{w}_i^{(t)}, \mathbf{W}_{-i}, \Theta_{-\mathbf{W}}^{r*}, \hat{\mathbf{Z}})} \frac{q(\mathbf{w}_i^* \rightarrow \mathbf{w}_i^{(t)})}{q(\mathbf{w}_i^{(t)} \rightarrow \mathbf{w}_i^*)},$$

where  $\mathbf{W}_{-i} = (\mathbf{w}_1, \dots, \mathbf{w}_{i-1}, \mathbf{w}_{i+1}, \dots, \mathbf{w}_p)$  and  $\Theta_{-\mathbf{W}}^{r*}$  is the parameter set for LSIRM except  $\mathbf{W}$ .

**2. Update the item difficulty parameter,  $\beta$ , of LSIRM.**

For  $i = 1, \dots, p$ ,

$$r(\beta_i^*, \beta_i^{(t)}) = \frac{\pi(\beta_i^*)}{\pi(\beta_i^{(t)})} \frac{P(\mathbf{X} | \beta_i^*, \beta_{-i}, \Theta_{-\beta}^{r*}, \hat{\mathbf{Z}})}{P(\mathbf{X} | \beta_i^{(t)}, \beta_{-i}, \Theta_{-\beta}^{r*}, \hat{\mathbf{Z}})} \frac{q(\beta_i^* \rightarrow \beta_i^{(t)})}{q(\beta_i^{(t)} \rightarrow \beta_i^*)},$$

where  $\beta_{-i} = (\beta_1, \dots, \beta_{i-1}, \beta_{i+1}, \dots, \beta_p)$  and  $\Theta_{-\beta}^{r*}$  is the parameter set for LSIRM except  $\beta$ .

**3. Update the person trait parameter,  $\theta$ , of LSIRM.** For  $k = 1, \dots, n$ ,

$$r(\theta_k^*, \theta_k^{(t)}) = \frac{\pi(\theta_k^*)}{\pi(\theta_k^{(t)})} \frac{P(\mathbf{X} | \theta_k^*, \theta_{-k}, \Theta_{-\theta}^{r*}, \hat{\mathbf{Z}})}{P(\mathbf{X} | \theta_k^{(t)}, \theta_{-k}, \Theta_{-\theta}^{r*}, \hat{\mathbf{Z}})} \frac{q(\theta_k^* \rightarrow \theta_k^{(t)})}{q(\theta_k^{(t)} \rightarrow \theta_k^*)},$$

where  $\theta_{-k} = (\theta_1, \dots, \theta_{k-1}, \theta_{k+1}, \dots, \theta_n)$  and  $\Theta_{-\theta}^{r*}$  is the parameter set for LSIRM except  $\theta$ .

**4. Update the variance parameter of the person trait parameter in LSIRM using Gibbs sampler.**

$$\pi(\sigma^2 | \cdot) \sim \text{IG}\left(a + \frac{1}{2}n, b + \frac{1}{2} \sum_{k=1}^n \theta_k^2\right)$$

5. **Update the social influence parameter,  $\delta$ .**

$$r(\delta^*, \delta^{(t)}) = \frac{\pi(\delta^*)}{\pi(\delta^{(t)})} \frac{P(\mathbf{X} | \delta^*, \Theta_{-\delta}^{r*}, \hat{\mathbf{Z}})}{P(\mathbf{X} | \delta^{(t)}, \Theta_{-\delta}^{r*}, \hat{\mathbf{Z}})} \frac{q(\delta^* \rightarrow \delta^{(t)})}{q(\delta^{(t)} \rightarrow \delta^*)}.$$

where  $\Theta_{-\delta}^{r*}$  is the parameter set for LSIRM except  $\delta$ .

For all data analysis shown in the current paper, we use the following values for the priors:  $\sigma_\alpha = \sigma_\beta = 2.5$ ,  $\sigma_\gamma = \sigma_\delta = 1.0$  and  $a_\sigma = b_\sigma = 0.001$ . For proposals, Gaussian proposal distributions are used which are centered at the current values of the parameters of the latent positions. The variances of the proposal distributions are set to have reasonable acceptance rates (around 0.2 - 0.5).

**Identification** The likelihood functions of the adapted LSIRM social influence are invariant to translations, reflections, and reflections as in standard latent space models (Hoff et al., 2002). As a result, the latent positions are not identifiable, while the distances are identifiable). However, this issue can be successfully resolved by post-processing the MCMC samples with Procrustes matching (Gower, 1975) as shown in the literature (Hoff et al., 2002; Jeon et al., 2021). In the two-step estimation of the adapted LSIRM, we apply Procrustes matching at the end of the LSM estimation (Step 1); then, the matched respondent positions are used for the estimation of the parameters of the adapted LSIRM in Step 2. At the end of Step 2, Procrustes matching is applied again to match the latent spaces from the Step 2 MCMC iterations. All Bayesian inferences are made with the matched posterior samples obtained after completing the Step 2 estimation and matching. To evaluate the convergence of the MCMC algorithm, we use trace plots along with Gelman-Rubin diagnostics (Gelman and Rubin, 1992). All code was written in R and C++ and available in the supplementary materials.

## 4 Real Data Application

### 4.1 Data

For an empirical illustration of the proposed approach, we used the data from the “Changing Climates of Conflict” study (Paluck et al., 2016). A large-scale field study was designed to measure the effects of anti-conflict interventions across 56 New Jersey public middle schools with 24,191 students in 2012 and 2013. For data analysis, we selected four schools based on students’ racial and economic backgrounds. Specifically, we chose School 35 with the highest percentage of white students (83% of 546 students) and School 45 with the highest percentage of Hispanic and African American students (82% of 329

students). In addition, we included School 59 with the second-lowest percentage of students receiving free or reduced lunch (11% of 539 students) and School 44 with the highest percentage of students receiving free or reduced lunch (69% of 241 students).<sup>1</sup>

Students were asked to write down their friends (up to ten) and their best friends (up to two) in school. We constructed a binary adjacency matrix per school from both their friends and best friends within a school; we refer to them *close friends* in this paper. Table 1 summarizes some characteristics of the schools selected for data analysis, including network summary statistics and average student background information.

	Nodes	Edges	Male	White	H/AA	F/R	LEP	CEN
School 36	546	3574	0.53	0.83	0.07	0.08	0.01	0.26
School 45	329	1907	0.51	0.04	0.82	0.65	0.04	0.38
School 44	241	1435	0.56	0.08	0.67	0.69	0.06	0.28
School 59	539	4204	0.48	0.74	0.11	0.11	0.02	0.32

Table 1: Some background characteristics of the four schools. Nodes (number of nodes(students)), edges (number of edges), male, White, H/AA (Hispanic and African American), F/R (free or reduced lunch), LEP (limited English proficiency) are the proportions in the students of the corresponding categories. CEN is the mean of eigenvector centrality, a measure of the influence of a node on a network. For the data being analyzed, if a student was pointed to by many other students (who were pointed by others), then the student has high eigenvector centrality. School 45 has the highest eigenvector centrality among the four schools.

In addition, the students were asked to indicate what school activities they participated in among the following ten activities: (1) sports within schools, (2) sports outside schools, (3) theater or drama, (4) music, (5) arts, (6) clubs in other schools, (7) dating within schools, (8) homework, (9) reading, and (10) video games. Figure 4 presents the histogram of the total number of activities reported in student response data per school. The distributions of the total number of school activities are fairly similar across the four schools. In all schools, two to four activities were most frequently observed. Table 2 shows the proportion of students participated in each school activity per school. Overall, Activity 2 (sports outside schools) and Activity 10 (video games) were the most frequently participated activities, while

<sup>1</sup>School 36 showed the lowest percentage of students receiving free or reduced lunch. Since School 36 was already selected, we chose School 44, the next one.

Activity 3 (theater/drama) and Activity 6 (clubs outside schools) were the least frequently participated activities in the four schools.

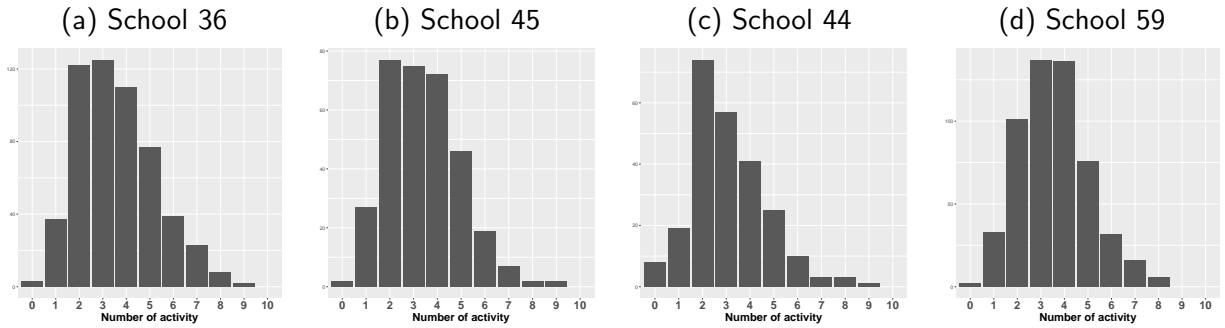


Figure 4: The histograms of the total number of activities that students were participating in.

Activity	1	2	3	4	5	6	7	8	9	10
School 36	6.64	21.86	2.45	10.88	5.72	5.72	9.40	13.43	7.51	16.39
School 45	6.42	15.43	5.62	11.69	7.76	1.69	7.49	10.53	8.74	24.62
School 44	9.58	18.49	2.56	8.64	6.75	1.89	5.53	9.99	9.04	27.53
School 59	13.84	20.71	2.13	8.69	3.12	5.41	6.97	16.08	6.97	16.08

Table 2: Percentage of the student participants in each activity per school. Activity 1 to 10 indicate participation in: (1) sports in school, (2) sports outside school, (3) theater/drama, (4) music, (5) arts, (6) clubs in other schools, (7) dating in school, (8) homework, (9) reading, and (10) video games.

## 4.2 Estimation

We applied the proposed approach to each school’s data to evaluate how their close friend network influenced their school activities. The MCMC algorithm was run for 60,000 iterations for each school dataset, with the first 10,000 iterations being discarded as a burn-in process. From the remaining 50,000 iterations, 10,000 samples were collected at a time-space of 5 iterations. Jumping rules for the proposal distributions are provided in the Supplementary Material.

For comparison, we additionally applied a linear network autocorrelation model (Leenders, 2002) as an alternative method to measure social influence. Specifically, the network autocorrelation regression model was set up with the counts of positive responses to the school activity items, representing the target behavior of interest, as the dependent variables and an adjacency matrix of a peer network as a weight for measuring the autocorrelation. Suppose for the binary behavior response data  $X_{k,i}$ , we define



$S_k = \sum_i X_{k,i}$ . Then we have

$$S_k = \rho \sum_{l \neq k} Y_{k,l} S_l + \epsilon_k, \quad \epsilon_k \sim N(0, \sigma^2),$$

where  $\rho$  is a network autocorrelation parameter that estimates the autoregression of each  $S_k$  value on its neighbors in the peer network, representing social influence. The network autocorrelation model was estimated using the `lnam` function in the `sna` package in R.

### 4.3 Results

**Overall Social Influence** Table 3 lists  $\delta$  parameter estimates from the proposed approach and the autocorrelation parameter of the network autocorrelation model for the four schools.

	Proposed approach			Network autocorrelation	
	Posterior Mean	95% HPD Interval		Coefficient	95% CI
School 36	0.826	( 0.680,	0.962)	0.063	( 0.061, 0.066)
School 45	-0.566	(-0.726,	-0.412)	0.068	( 0.065, 0.073)
School 44	0.496	( 0.279,	0.702)	0.066	( 0.062, 0.071)
School 59	1.040	( 0.865,	1.212)	0.056	( 0.054, 0.058)

Table 3: Posterior mean and 95% HPD intervals of the influence parameters for School 36, 45, 44, and 59.

Our approach suggests that overall social influence was present in all four schools, although there was some difference in the size and the direction. In Schools 59, 36, and 44, overall social influence effects were positive, meaning that the students' close friend network increased their likelihood of participating in school activities. Interestingly, in School 45, with the highest proportion of Hispanic/African American students, as the latent positions between pairs of students get closer, the likelihood of participating in activities of interest together tends to decrease. School 59 showed stronger social influence than other schools, and the influence size of School 44 was about half of School 59. Note that all autocorrelation parameters estimated from the network autocorrelation model are small but positive (CIs do not include zero) and similar across the four schools. The size of our overall social influence parameter  $\delta$  and the autocorrelation parameter  $\rho$  may not be directly comparable because of the difference in the unit of analysis; our model analyzes the item-level binary behavior data, whereas the network autocorrelation model analyzes the scale-level continuous behavior data. Plus, the way how social influence is defined

in the two models. It is also worth mentioning that we offer the latent space, which reveals a detailed picture of social influence and the parameter  $\delta$  that quantifies the overall size of social influence.

**Latent Space** Here we describe the estimated latent spaces of the four schools, which show detailed pictures of social influence, i.e., how students' social network influences their behavior.

Figure 5 displays the adapted latent space of School 36, 45, 44, and 59. Student locations and grouping describe the structure of close friend networks in each school. Item positions are determined to reflect activity similarities of close friends (who are close to each other in the latent space). This means that depending on the characteristics of close friends, item positioning and clustering structures could be different in different schools.

In School 39, with the highest percentage of White students, we observe roughly two groups of respondents in the space, meaning that students belong to one of the two close friend networks in this school. There are roughly three item groups in the space. Activities 1 (sports in school), 2 (sports outside school), 6 (clubs in other schools), and 7 (dating) positioned near the center of the space make one group, and students neighboring those items from the two student clusters had a higher likelihood of participating in the corresponding activities. Activities 3 (theater/drama), 4 (music), 5 (arts), 8 (homework), and 9 (reading) positioned in the bottom of the space make another group, and students neighboring those items had a higher likelihood of participating in the corresponding activities. Interestingly, the first and second item groups represent physical and non-academic vs. non-physical and academic activities, respectively. Activity 10 (video games) made the third group were further away from the second item group (non-physical and academic) more than the first item group (physical and non-academic).

In School 45, with the highest percentage of Hispanic/African American students, we observe one student cluster only, meaning that students' close friend network was not really divided in this school. The activity items were, however, divided into three groups. One group located at the bottom of the space includes Activities 1 (sports in school), 2 (sports outside school), 7 (dating), and 10 (video games). The second item group located a little above the center includes Activities 5 (arts), 6 (clubs in other schools), 8 (homework), and 9 (reading). The third item group is located at the top of the space and includes Activities 3 (theater/drama) and 4 (music). Interestingly, video games (Activity 10) is related to physical activities such as sports, and club activities in other schools (Activity 6) is close to academic activities such as homework in this school. Note that the influence parameter  $\delta$  had a negative sign in School 45, meaning that being close to certain activities indicates a lower likelihood of participating

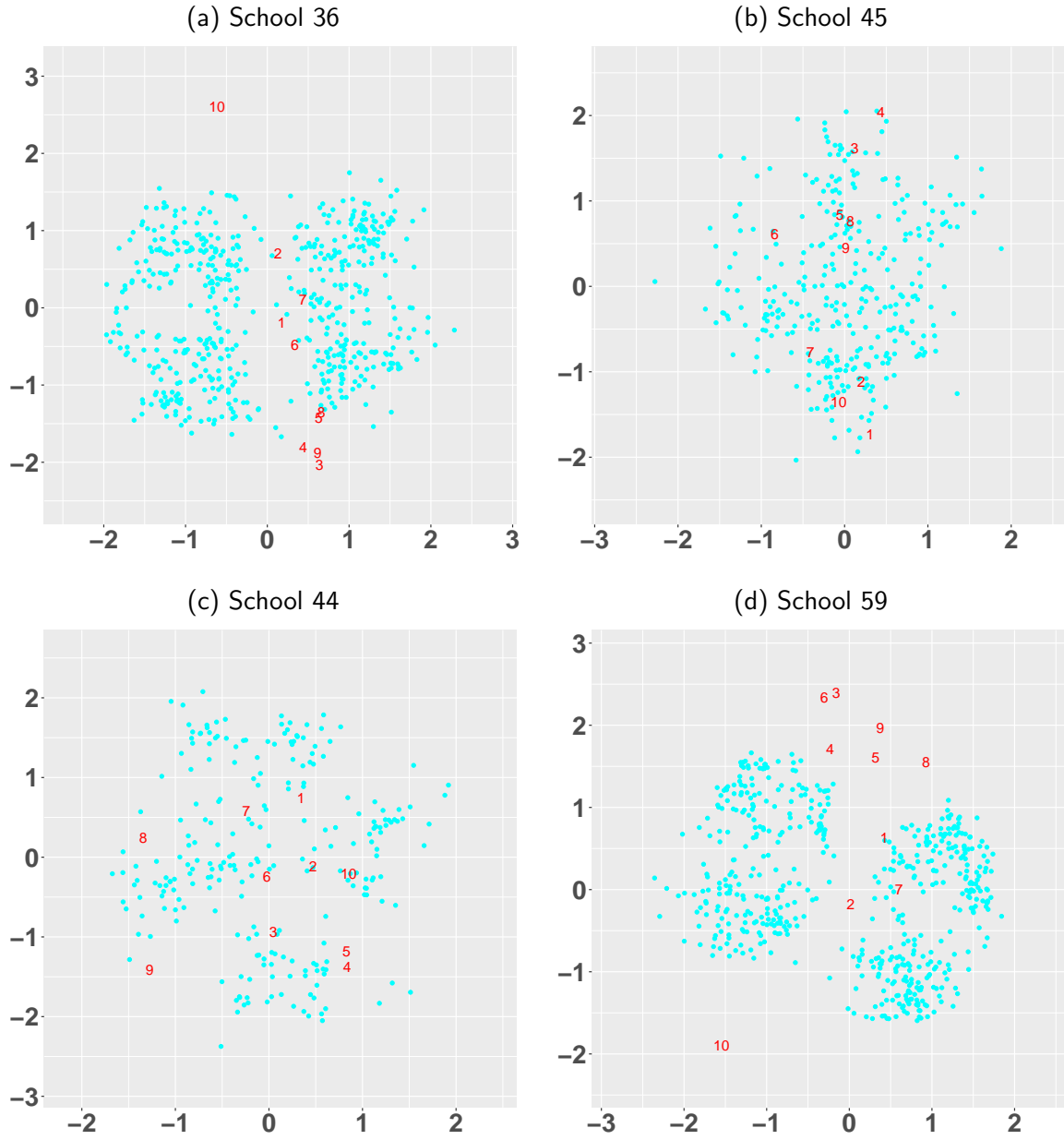


Figure 5: Latent spaces for School 36, 45, 44 and 59. School 36 has the highest percentage of White students, and School 45 has the highest percentage of Hispanic/African American students. School 44 and School 59 have the highest and lowest percentage of low-income students, respectively.

in them, not a higher likelihood as in other schools. For example, students near the item group in the bottom region (Activities 1, 2, 7, 10) tended to show a lower likelihood of those activities.

In School 44, with a high percentage of low-income and limited English proficiency students, we observe roughly four student clusters (top, bottom, left, and right sides of the space), although the distinction is somewhat fuzzy. Item grouping is not clear either, although items are located in different areas of the space. We can identify which items each friendship cluster is closest to. This information helps us understand what activities the friend groups share. For example, the friend group on the bottom is close to Activities, 3 (theater/drama), 4 (music), and 5 (arts). On the other hand, the friend group on the top are closer to Activities 1 (sports in school) and 7 (dating) than other activities, while the friend group on the right is close to Activities 2 (sports outside school) and 10 (video games).

In School 59, with a low percentage of low-income students, we see roughly two clusters and three item groups as in school 36. Item grouping is also quite similar to the grouping shown in School 36 with similar student characteristics. For example, the item group near the center includes Activities 1, 2, and 7. The group on the top includes Activities 3, 4, 5, 6, 8, and 9. The only difference is that Activity 6 (clubs in other schools) is more closely associated with non-physical/academic activity groups than physical/non-academic activities in this school. Activity 10 (video games) is further away from the two item groups as in School 59. Interestingly, School 59 and School 36 are very similar in student characteristics, and such similarity is also reflected in the student activities of close friends.

As described above, the adapted latent spaces help us understand the structure of the student network and how the student network is related to their school activities. If desirable, one can take a closer look at the shared school activities of individual students and their close friends by evaluating the distance to the activity items.

**Other Parameter Estimates** Figures 6 summarize the posterior samples of all model parameters in the four schools. The top row compares the parameter estimates between Schools 36 and 45, and the bottom row compares schools 44 and 59.  $\alpha$  and  $\gamma$  are the intercepts and weight parameters (for LSM) in Step 1.  $\beta_i$  and  $\delta$  are the item easiness and social influence parameters (for LSIRM) in Step 2, respectively. In the top row comparison, School 36 (red) has a larger  $\alpha$  and  $\gamma$  parameter values than School 45 (blue), which means students in School 36 tended to report more close friends than students in School 45. Both  $\beta_i$  and  $\delta$  parameter estimates are higher in School 36 than in School 45. A large influence of the friendship network on school activities leads to an increased easiness level of individual school activities. School 45 has the highest percentage of Hispanic/African American students, and School 36 has the highest

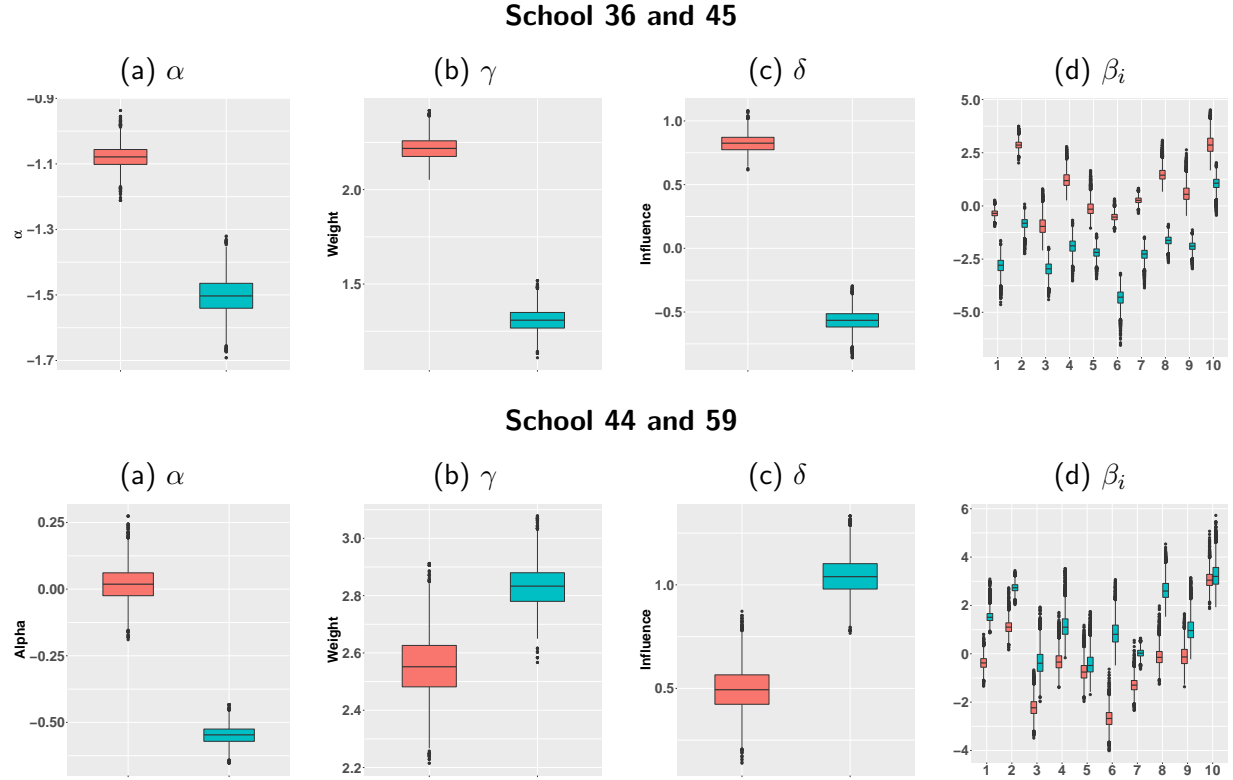


Figure 6: Boxplots of the posterior samples of the model parameters in four schools. In the top row, red is School 36, blue is School 45. In the bottom row, red is School 44, and blue is School 59.  $\alpha$  and  $\gamma$  are the intercept and weight parameters of the Step 1 model.  $\delta$  and  $\beta_i$  are the social influence and item easiness parameter of the Step 2 model, respectively.

percentage of White students. As mentioned earlier, the social influence parameter  $\delta$  was estimated negative in School 45, indicating that having many close friends was associated with decreased rates of participating in school activities in the School with the highest percentage of Hispanic/African American students.

In the second row comparison, School 44 (red) has a larger  $\alpha$  value than School 59 (blue), meaning that students in School 44 tend to report more close friends than School 59. However, the weight  $\gamma$  was slightly smaller in School 44 than in School 59, indicating that students in School 59 tend to have more diverse friendships than those in School 44. School 44 showed smaller  $\delta$  and  $\beta_i$  than School 59. In School 44, with more low-income students than school 59, having many close friends did not necessarily increase the students' participation in school activities.

## 5 Simulation Studies

We conducted simulation studies to examine the performance of the proposed approach in various data generating conditions. We focused on evaluating (1) the social influence parameter ( $\delta$ ) and (2) the overall model fit of the proposed modeling approach. Details of the study design, method, and results are provided in this section.

### 5.1 Study Design

We generated binary social network data of friendship  $\mathbf{Y}_{n \times n}$  and binary item-level behavior data  $\mathbf{X}_{n \times p}$  under our proposed modeling framework. We considered five different latent space configurations, where respondents' latent space configuration based on response behavior matched their social network space configuration in Scenarios 1.1 to 1.3, while the two latent space configurations mismatch to some extent in Scenarios 2 and 3. We separately generated  $\alpha$ ,  $\beta = \{\beta_i\}_{i=1}^p$ , and  $\theta = \{\theta_k\}_{k=1}^n$  from Uniform (-1, 1) for each dataset in all scenarios. We fix the weight parameter  $\gamma = 1$  and set the social influence parameter  $\delta = 1$ . The latent space configuration in the five scenarios are described in detail below.

**Scenario 1.1** We need to consider two latent spaces, one for a social network and the other for a respondent-item network. For the social network space, we assume there are three clusters that include 100 people per cluster. For the item-respondent network space, we consider three-person clusters, same as the social network space, as well as three-item clusters with ten items per cluster. As shown in Figure 7(a), one person cluster is associated with one item cluster such that: (1) respondents in Cluster 1

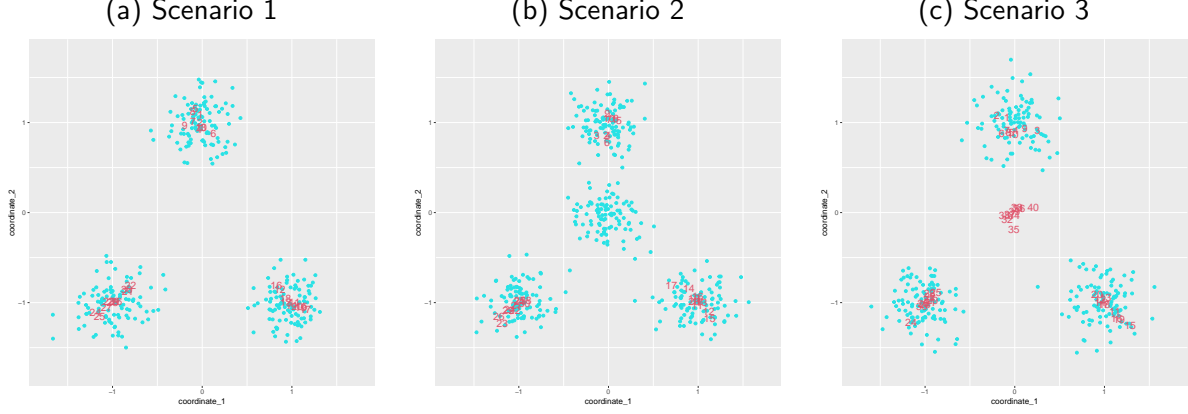


Figure 7: Latent spaces that illustrate Scenario 1.1 to 1.3. Red numbers and blue dots represent the latent positions of items and respondents, respectively.

(respondents 1-100) tend to give positive answers to item group 1 only (items 1 - 10); (2) respondents in Cluster 2 (respondents 101-200) tend to give positive responses to item group 2 only (items 11 - 20); and (3) respondents in Cluster 3 (respondents 201-300) tend to give positive answers to item group 3 only (item 21 - 30). In this basic scenario, the person clusters from the social network space exactly match the person clusters from the item-response network. That is, people with only similar response behavior are assumed to be friends with each other in this scenario.

Under this setting, we generated the latent positions of individuals ( $n = 300$ ) and behavior items ( $p = 30$ ) as follows:

$$\mathbf{z}_k = \sum_{g=1}^3 N(\boldsymbol{\mu}_g, \boldsymbol{\Sigma}_z) I(g_k = g) \quad \text{and} \quad \mathbf{w}_i = \sum_{g=1}^3 N(\boldsymbol{\mu}_g, \boldsymbol{\Sigma}_{w,g}) I(g_i = g), \quad (10)$$

where  $\mathbf{z}_k$  and  $\mathbf{w}_i$  are the positions of individual  $k$  and item  $i$ , and  $g_k$  and  $g_i$  are the cluster/group membership for respondent  $k$  and item  $i$ , where  $k = 1, 2, 3$  and  $i = 1, 2, 3$ . The group means and co-variances were set to as follows:

$$\boldsymbol{\mu}_1 = \begin{pmatrix} 0 \\ 1 \end{pmatrix}, \quad \boldsymbol{\mu}_2 = \begin{pmatrix} 1 \\ -1 \end{pmatrix}, \quad \boldsymbol{\mu}_3 = \begin{pmatrix} -1 \\ -1 \end{pmatrix}, \quad (11)$$

and

$$\begin{aligned} \boldsymbol{\Sigma}_z &= \begin{pmatrix} 0.2^2 & 0 \\ 0 & 0.2^2 \end{pmatrix}, \quad \boldsymbol{\Sigma}_{w,1} = \begin{pmatrix} 0.1^2 & 0 \\ 0 & 0.1^2 \end{pmatrix}, \\ \boldsymbol{\Sigma}_{w,2} &= \begin{pmatrix} 0.1^2 & -0.9 \cdot 0.1^2 \\ -0.9 \cdot 0.1^2 & 0.1^2 \end{pmatrix}, \quad \boldsymbol{\Sigma}_{w,3} = \begin{pmatrix} 0.1^2 & 0.9 \cdot 0.1^2 \\ 0.9 \cdot 0.1^2 & 0.1^2 \end{pmatrix}. \end{aligned} \quad (12)$$

Details of generating the simulation data for Scenario 1.1 are described in Algorithm 1 of the Supplementary Materials.

**Scenario 1.2** In Scenario 1.2, we consider four-person clusters for the social network space that include 100 people per cluster. For the item-responder network space, we consider four-person clusters and three-item clusters. As shown in Figure 7(b), Scenario 1.2 is identical to Scenario 1.1 except for the fourth person cluster in the middle of the space.

$\mu_1, \mu_2, \mu_3, \Sigma_z$  and item clusters that are identical to Scenario 1.1 were generated based on Equation (10). The group mean of the fourth person cluster was set as  $\mu_4 = (0, 0)^T$ . Then, we generate the latent positions of individuals ( $n = 400$ ) as follows:

$$\mathbf{z}_k \sim \sum_{g=1}^4 N(\mu_g, \Sigma_z) I(g_k = g).$$

**Scenario 1.3** In Scenario 1.3, we consider three-person clusters for the social network space as in Scenario 1.1. For the item-responder network space, we consider three-person clusters and four-item clusters as displayed in Figure 7(c). Scenario 1.3 is identical to Scenario 1.1 except for the fourth item cluster in the middle of the space.

We generated the three person clusters that are identical to Scenario 1.1 based on Equation (10).  $\mu_1, \mu_2, \mu_3, \Sigma_{w,1}, \Sigma_{w,2}$ , and  $\Sigma_{w,3}$  are also identical to Equation (10) in Scenario 1.1. The group mean and co-variance for the fourth item cluster was set as

$$\mu_4 = \begin{pmatrix} 0 \\ 0 \end{pmatrix} \quad \text{and} \quad \Sigma_{w,4} = \begin{pmatrix} 0.1^2 & 0 \\ 0 & 0.1^2 \end{pmatrix}.$$

Moreover, we generated the latent positions of item ( $p = 40$ ) as follows:

$$\mathbf{w}_i \sim \sum_{g=1}^4 N(\mu_g, \Sigma_{w,g}) I(g_k = g).$$

**Scenario 2** Unlike Scenarios 1.1 to 1.3, we now assume that the social network space configuration mismatches the item-responder network configuration. Specifically, for the social network, we consider two-person clusters (150 respondents per cluster), while three-person clusters (100 people per cluster) and three-item clusters (10 items per cluster) in the item-responder network. As displayed in Figures 8(a) and (b), the social network space appears quite different from the item-responder network space, such that the person cluster in the bottom of the space does not match any of the person clusters in the item-responder space.



## Scenario 2

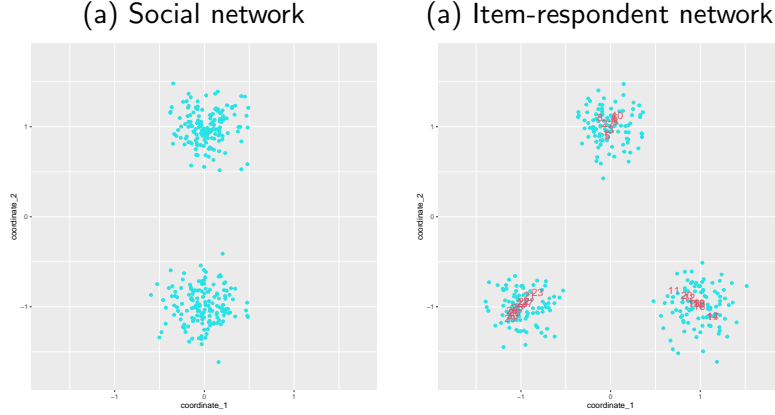


Figure 8: Social network latent space (a) and item-responsive latent space (b) considered in Scenario 2. Red numbers and blue dots represent latent positions for items and respondents, respectively.

The person and item positions of the item-responsive space were generated based on Eq (10). For the social network data, the latent position  $\mathbf{z}'_k$  for respondent  $k$  were generated as follows:

$$\mathbf{z}'_k \sim \sum_{g=1}^2 N(\boldsymbol{\mu}_{z'_g}, \boldsymbol{\Sigma}_{z'}) I(g_k = g),$$

where

$$\boldsymbol{\mu}_{z',1} = \begin{pmatrix} 0 \\ 1 \end{pmatrix}, \boldsymbol{\mu}_{z',2} = \begin{pmatrix} 0 \\ -1 \end{pmatrix}, \text{ and } \boldsymbol{\Sigma}_{z'} = \begin{pmatrix} 0.2^2 & 0 \\ 0 & 0.2^2 \end{pmatrix}.$$

Details of how to generate the simulation data for Scenario 2 are described in Algorithm 2 of the Supplementary Materials.

**Scenario 3** As in Scenario 2, we assume the latent space configurations are different in the two network spaces. For the social network, we assume three-person clusters as in Scenario 1.1. For the item-responsive network, we consider three-person clusters and three-item clusters. However, this time, the person clustering structure varies across several sub-conditions, as illustrated in Figure 9. Specifically, the person positions are determined as  $\mathbf{z}_k^* = \lambda \mathbf{z}_k$ , where  $\mathbf{z}_k$  is the person latent position from the network and  $\lambda$  determines the closeness of the clusters that can be interpreted as the effect of network to item response data. We consider  $\lambda = (0.01, 0.05, 0.1, 0.2, 0.4, 0.6, 0.8, 1.0)$ . When  $\lambda = 1$ , the person clusters are distinguished, and a dependent structure in a network apparently influences the respondent-item interactions. When  $\lambda = 0.01$ , the item clusters are nearly indistinguishable, and a network-dependent structure has the least effect on the respondent-item interactions. The prob-

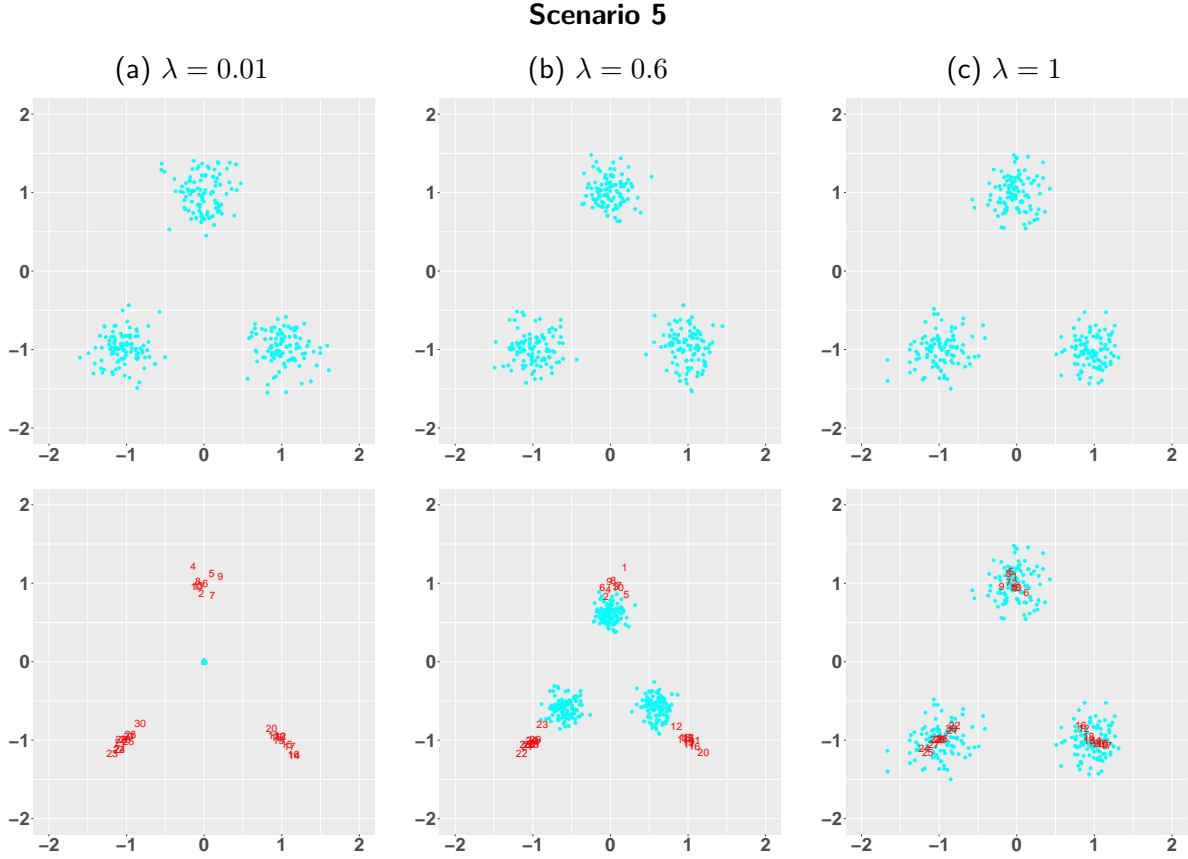


Figure 9: The top and bottom row are social network latent space and item response latent space for Scenario 3 of  $\lambda = 0.01, 0.6$  and  $1$ , respectively.

ability of answering items positively totally depends on the item difficulty and person characteristic parameters regardless of the dependent structures in a network.  $\lambda = 1$  gives the condition equivalent to Scenario 1. Details of generating the simulation data for Scenario 3 are described in Algorithm 3 of the Supplementary Materials.

**Summary** Scenarios 1.1 to 1.3 show that the latent space configuration and individuals' latent positions are the same in the spaces for item responses and social network data. Scenario 1.1 is the simplest setting where the number of person groups is the same as the number of items. This is no longer true in Scenarios 1.2 and 1.3. In Scenarios 2 and 3, the latent space configuration is not the same in the social network and item-responder networks. In Scenario 2, the number of person groups in the social network space is smaller than those in the item response space. In Scenario 3, the number of person groups is the same in the two spaces, but we control the influence of network dependence structure on responder-item dependent structure. Note that there is no change in item-item dependent structures in Scenario 2 and

3.

## 5.2 Estimation

Per scenario, 200 datasets were generated. For each simulated dataset, we applied the proposed approach to estimate the social influence parameter with the MCMC algorithm described in Section 3.2. We used 30,000 iterations, with the first 5,000 iterations being discarded as a burn-in process. From the remaining 25,000 iterations, 5,000 samples were collected at a time-space of 5 iterations. We adjusted the jumping rules for proposal distributions to achieve ideal acceptance rates (20% to 40%), identical to those in real data analysis. Details of the jumping rules are given in the Supplementary Material.

## 5.3 Social Influence Parameter Evaluation

Here we focused on evaluating the overall social influence parameter ( $\delta$ ) of the proposed approach. As a comparison, we additionally applied the network autocorrelation model that we used in the empirical study to measure social influence effects as the autocorrelation coefficients of the corresponding covariates per scenario. We also evaluated an additional model parameter for the proposed approach to discuss and provide additional evidence of estimation accuracy. To this purpose, we chose the  $\gamma$  parameter, the weight of the distance term of the LSM in Step 1 for two reasons: (1)  $\gamma$  is similar to  $\delta$  in that both are the weights of the distance terms, and (2) since  $\gamma$  is a parameter of the Step 1 estimation, we can discuss the accuracy of Step 1 estimation.

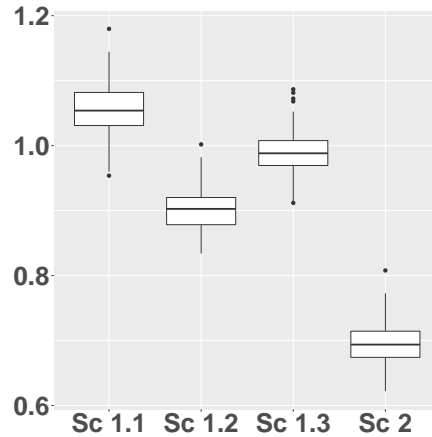


Figure 10: The boxplot of the posterior means of weight,  $\gamma$ , in Scenarios 1.1 - 2.

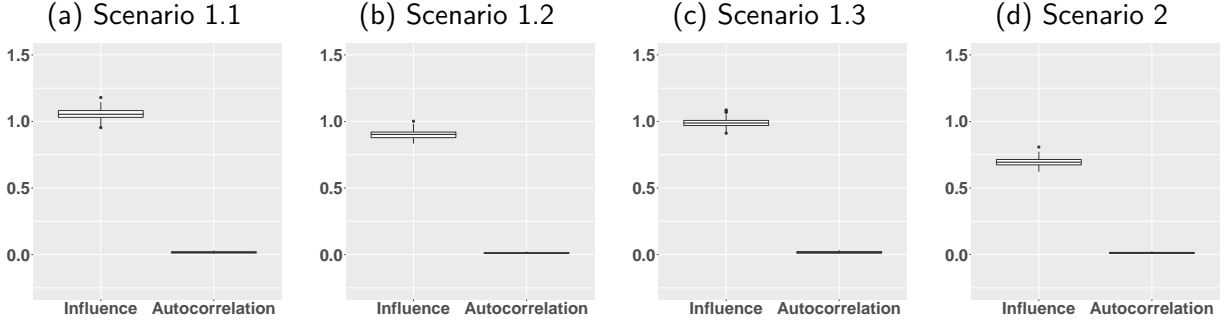


Figure 11: The boxplots of the posterior means of influence parameters, and autocorrelation coefficients in Scenarios 1.1 - 2.

**Scenarios 1.1–1.3 and 2** Figure 11 displays the boxplots of the posterior means of interesting parameters in Scenarios 1.1 to 1.3 and 2 over 200 replicates. Table 4 lists the mean and five-number summaries of the posterior means of the social influence parameters from the proposed approach over the 200 replicates.

	min	25%	median	75%	max	mean
Scenario 1.1	0.954	1.031	1.054	1.082	1.180	1.056
Scenario 1.2	0.834	0.878	0.903	0.920	1.002	0.902
Scenario 1.3	0.912	0.969	0.988	1.008	1.087	0.989
Scenario 2	0.622	0.674	0.694	0.714	0.808	0.695

Table 4: Mean and five-number summaries of the estimated posterior means for the social influence parameters from 200 simulated datasets for Scenario 1.1–2

The figure 10 shows that the weight parameter ( $\gamma$ ) was estimated with satisfactory precision in all four scenarios (the mean was close to the data generating value of 1.0). In Scenarios 1.1 to 1.3, the mean of estimated posterior means of the social influence parameter ( $\delta$ ) was close to 1.0, the data generating value. It is worth repeating that the person positions exactly match the social network and item-responder network in Scenarios 1.1 to 1.3. Therefore, the satisfactory recovery of the  $\delta$  and  $\gamma$  parameters ensures that the proposed estimation procedure operates appropriately.

The precision slightly decreased in Scenario 2 with the range of [0.62, 0.81] and the mean of 0.695. A lower precision is expected because the two latent space configurations mismatch in Scenario 2. Despite the high level of intentional mismatch between the social network and item-response networks,

the proposed approach was able to catch the impact of respondents' social network on their item-level behavior.

Estimated autocorrelation parameters for Scenario 1.1 to 1.3 and 2 from the network autocorrelation models were (0.017, 0.012, 0.013, 0.017). It is intriguing to note that the estimated autocorrelation parameters do not vary significantly, although there exist distinct differences in the dependent structures in each scenario. This implies that the network autocorrelation models could not catch social influence effects (as defined in our study) in the considered scenarios.

$\lambda$	min	25%	median	75%	max	mean
1.00	0.954	1.031	1.054	1.082	1.180	1.056
0.80	0.843	0.895	0.913	0.933	0.994	0.914
0.60	0.629	0.696	0.717	0.735	0.799	0.716
0.40	0.444	0.505	0.527	0.546	0.612	0.526
0.20	0.216	0.298	0.324	0.349	0.398	0.323
0.10	0.129	0.208	0.236	0.265	0.318	0.235
0.01	0.118	0.190	0.209	0.227	0.325	0.209

Table 5: Mean and five-number summary of the estimated posterior means for the social influence parameters from simulated datasets in Scenario 3.

**Scenario 3** As in Scenario 2, the social network and item-responder network mismatch in Scenario 3. Here we examined what happened when the degree of influence from network-dependent structure decreased (or the degree of mismatch increased) as  $\lambda$  decreases from 1.0 to 0.01. Figure ?? shows (a) the boxplots of the posterior means of the social influence parameters over the 200 replicates from the proposed approach and (b) the boxplots of the maximum likelihood estimates from the network autocorrelation model. Table 5 lists the mean and the five-number summary of the  $\delta$  parameter estimates in the sub-conditions of varying  $\lambda$ .

Overall, the precision of the social influence parameter estimates decreased as the influence decreased (i.e.,  $\lambda$  decreased from 1 to zero). When  $\lambda = 0.6$ , the  $\delta$  estimates had a range of [0.63, 0.80] with a mean of 0.72, which is similar to Scenario 1. When  $\lambda < 0.6$ , the  $\delta$  estimates became further away from the data generating value, 1.0. However, even when the influence was minimized with  $\lambda = 0.01$ , the 95% HPD of  $\delta$  never included zero in all 200 replicates. On the other hand, from the network autocorrelation model, the autocorrelation parameter estimates did not vary significantly by the value of  $\lambda$ , meaning

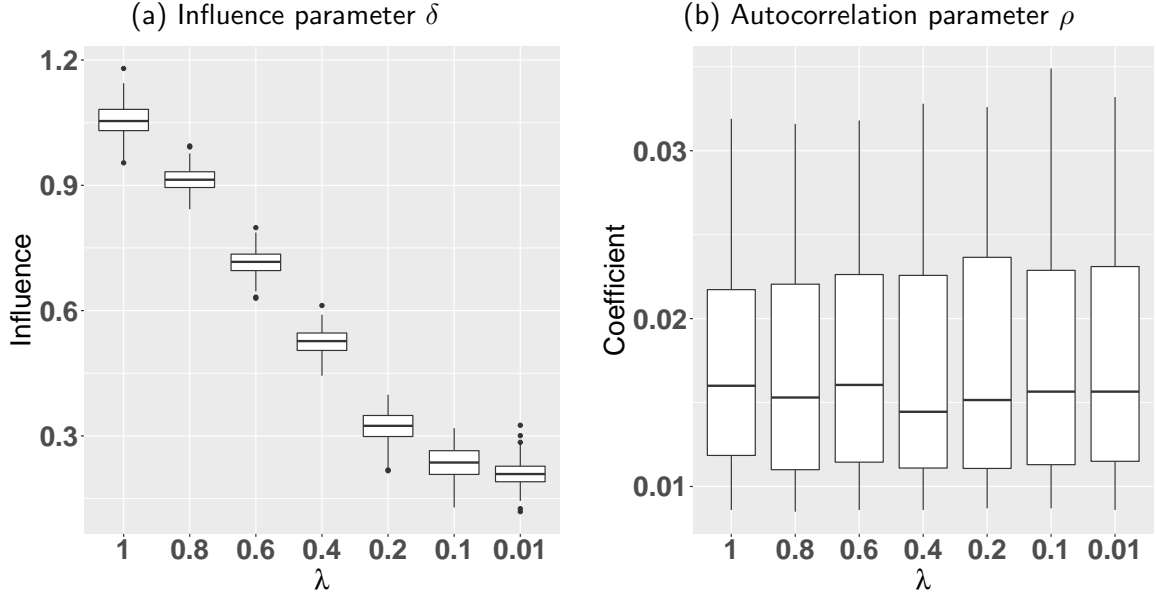


Figure 12: Boxplots of the social influence parameter estimates from (a) the proposed approach and (2) the network autocorrelation approach over 200 replicates by  $\lambda$  in Scenario 5.

that, in Scenario 3, the network autocorrelation model cannot distinguish the effects of the influences from different degrees of mismatch.

#### 5.4 Model Fit Evaluation

We evaluated the absolute fit of the proposed approach in simulated data. We chose Scenario 3 that includes both conditions with match ( $\lambda = 1$ ) and no match ( $\lambda < 1$ ) between the social network and the item-response network. To evaluate the goodness-of-fit of the proposed model, we assessed differences between the true and estimated probabilities of the positive responses,  $p_{r,ki} - \hat{p}_{r,ki}$  in all  $\lambda$  conditions, where

$$p_{r,ki} = \frac{\exp(\beta_i + \theta_k - \delta \|\hat{\mathbf{z}}_k - \mathbf{w}_i\|)}{1 + \exp(\beta_i + \theta_k - \delta \|\hat{\mathbf{z}}_k - \mathbf{w}_i\|)}.$$

Figure 13 shows the boxplots and Table 6 lists the five number summaries of  $p_{r,ki} - \hat{p}_{r,ki}$  over 200 replicates. In all  $\lambda$  conditions, the discrepancies are minimal, indicating that the goodness of fit of the proposed approach was satisfactory even when the estimating model was different from the data generating model (mismatch conditions of  $\lambda < 1$ ).

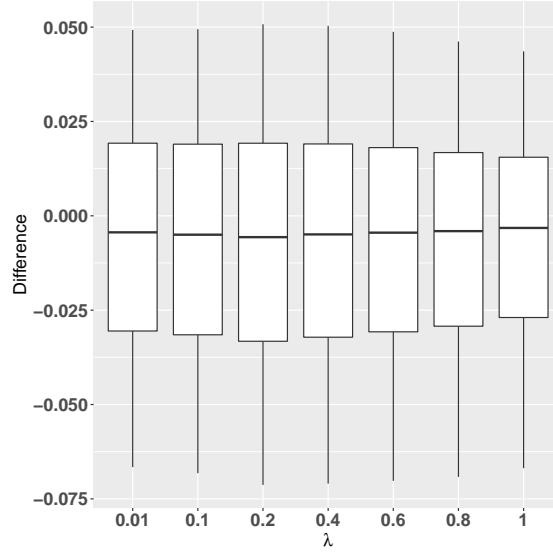


Figure 13: boxplot of  $p_{r,ki} - \hat{p}_{r,ki}$  for the social influence model. As the differences get close to 0, the performance of the model is better.

$\lambda$	min	25%	median	75%	max	mean
0.01	-0.499	-0.053	-0.004	0.038	0.454	-0.008
0.10	-0.451	-0.054	-0.005	0.038	0.424	-0.009
0.20	-0.467	-0.057	-0.006	0.039	0.458	-0.010
0.40	-0.472	-0.056	-0.005	0.038	0.485	-0.010
0.60	-0.492	-0.055	-0.004	0.037	0.466	-0.010
0.80	-0.512	-0.053	-0.004	0.034	0.520	-0.011
1.00	-0.550	-0.051	-0.003	0.032	0.562	-0.011

Table 6: Mean and five-number summaries of  $p_{r,ki} - \hat{p}_{r,ki}$  of the social influence model.

## 6 Discussion

We have introduced a new approach for assessing the influence of individuals' social networks on their behavior. In our proposed model, evaluating social influence comes down to the task of integrating two latent space models, one for network and the other for item-level behavior data. Specifically, our social influence model estimates interactions in item response data given the respondent's latent positions from a network. The adapted latent space estimated from the proposed approach shows the structure and patterns of social influence in the data, while the overall magnitude and direction of social influence can be evaluated by the weight parameters of the distance terms in latent space models. We developed a fully Bayesian approach to estimate the proposed model and illustrated the proposed approach with an empirical data example. We conducted simulation studies to understand the operating characteristics of our proposed model and evaluate the performance of our proposed approaches. Our approach is the first attempt to explain social influence with network and item-level behavior data.

Before closing, we would like to make three remarks. First, our proposed social influence model is designed for cross-sectional network data. However, our modeling framework can be extended to longitudinal data by incorporating recently developed latent space model for dynamic unipartite networks (Sewell and Chen, 2015; Loyal and Chen, 2020) and bipartite networks (Friel et al., 2016). Second, a related study by Wang et al. (2019) on a joint attribute and person latent space model (APLSM) summarizes information from social network and item-level data in a joint latent space. Both models allow modeling social network and item response data simultaneously using a latent space modeling approach. However, APLSM and our social influence model show significant differences in their analytical purposes. APLSM assumes the joint latent space for network and item response and explains item-item, person-person, and person-item interactions. On the other hand, our social influence model estimates the degree of the influence from the network to item response under the latent space modeling framework. Lastly, our proposed model is a regression-based approach, and therefore the results should be treated as the association between networks and behavior rather than as a study of causal effects. Nevertheless, it still remains an interesting topic to describe how students' social interactions are related to their behavior.

## Acknowledgements

This work was supported by Yonsei University Research Fund [grant number 2019-22-0210 awarded to IHJ] and the National Research Foundation of Korea [grant number NRF 2020R1A2C1A01009881;



Basic Science Research Program awarded to IHJ].

## References

- Berlusconi, G., A. Aziani, and L. Giommoni (2017, 03). The determinants of heroin flows in europe: A latent space approach. *Social Networks*.
- Cheng, L. A., G. Mendonça, and J. C. d. Farias Júnior (2014). Physical activity in adolescents: analysis of the social influence of parents and friends. *Jornal de Pediatria* 90(1), 35–41.
- Daraganova, G. and G. Robins (2013, 01). Autologistic actor attribute models. *Exponential Random Graph Models for Social Networks: Theory, Methods and Applications*, 102–114.
- Dittrich, D., R. T. A. J. Leenders, and J. Mulder (2019). Network autocorrelation modeling: A bayes factor approach for testing (multiple) precise and interval hypotheses. *Sociological Methods & Research* 48(3), 642–676.
- Doreian, P. (1980). Linear models with spatially distributed data: Spatial disturbances or spatial effects? *Sociological Methods & Research* 9(1), 29–60.
- Doreian, P. (1982). Maximum likelihood methods for linear models: Spatial effect and spatial disturbance terms. *Sociological Methods & Research* 10(3), 243–269.
- Doreian, P. (1989). Network autocorrelation models: Problems and prospects. In D. Griffith (Ed.), *Spatial Statistics: Past, Present, Future*. Ann Arbor: Michigan Document Services.
- Dow, M. M., M. L. Burton, and D. R. White (1982). Network autocorrelation: A simulation study of a foundational problem in regression and survey research. *Social Networks* 4(2), 169–200.
- Erdős, P. and A. Rényi (1960). On the evolution of random graphs. *Publications of the Mathematical Institute of the Hungarian Academy of Sciences* 5, 17–61.
- Fienberg, S. E. (2012). A brief history of statistical models for network analysis and open challenges. *Journal of Computational and Graphical Statistics* 21, 825–839.
- Frank, K. A., Y. Zhao, and K. Borman (2004). Social capital and the diffusion of innovations within organizations: The case of computer technology in schools. *Sociology of Education* 77(2), 148–171.

- Friel, N., R. Rastelli, J. Wyse, and A. E. Raftery (2016). Interlocking directorates in Irish companies using a latent space model for bipartite networks. *Proceedings of the National Academy of Sciences of the United States of America* 113, 6629–6634.
- Fujimoto, K., P. Wang, and T. W. Valente (2013). The decomposed affiliation exposure model: A network approach to segregating peer influences from crowds and organized sports. *Network Science* 1(2), 154–169.
- Gelman, A. and D. B. Rubin (1992). Inference from iterative simulation using multiple sequences. *Statistical Science* 7, 457–472.
- Gollini, I. and T. B. Murphy (2016). Joint modeling of multiple network views. *Journal of Computational and Graphical Statistics* 25, 246–265.
- Gower, J. C. (1975). Generalized procrustes analysis. *Psychometrika* 40(1), 33–51.
- Handcock, M. S., A. E. Raftery, and J. M. Tantrum (2007). Model-based clustering for social network. *Journal of the Royal Statistical Society, Series A* 170, 301–354.
- Hoff, P., A. Raftery, and M. S. Handcock (2002). Latent space approaches to social network analysis. *Journal of the American Statistical Association* 97, 1090–1098.
- Hunter, D. (2007). Curved exponential family models for social networks. *Social networks* 29, 216–230.
- Jeon, M., I. H. Jin, M. Schweinberger, and S. Baugh (2021). Mapping unobserved item-responder interactions: A latent space item response model with interaction map. *Psychometrika In Press*, 1–38.
- Krivitsky, P. N., M. S. Handcock, A. E. Raftery, and P. D. Hoff (2009). Representing degree distributions, clustering, and homophily in social networks with latent cluster random network models. *Social Networks* 31, 204–213.
- Leenders, R. T. (2002). Modeling social influence through network autocorrelation: constructing the weight matrix. *Social Networks* 24(1), 21–47.
- Liu, H., I. H. Jin, Z. Zhang, and Y. Yuan (2020). Social network mediation analysis: A latent space approach. *Psychometrika* 86, 272–298.
- Loyal, J. D. and Y. Chen (2020). A bayesian nonparametric latent space approach to modeling evolving communities in dynamic networks. *arXiv preprint arXiv:2003.07404*.

- Mercken, L., T. A. Snijders, C. Steglich, E. Vertainen, and H. D. Vries (2010). Smoking-based selection and influence in gender-segregated friendship networks: a social network analysis of adolescent smoking. *Addiction* 105, 1280 – 1289.
- Ord, K. (1975). Estimation methods for models of spatial interaction. *Journal of The American Statistical Association* 70, 120–126.
- Paluck, E. L., H. Shepherd, and P. M. Aronow (2016). Changing climates of conflict: A social network experiment in 56 schools. *Proceedings of the National Academy of Sciences of the United States of America* 113, 566–571.
- Parker, A., F. Pallotti, and A. Lomi (2021). New network models for the analysis of social contagion in organizations: An introduction to autologistic actor attribute models. *Organizational Research Methods* 24, 10944281211005167.
- Raftery, A., X. Niu, P. Hoff, and K. Yeung (2012). Fast inference for the latent space network model using a case-control approximate likelihood. *Journal of Computational and Graphical Statistics* 21, 909–919.
- Rastelli, R., N. Friel, and A. Raftery (2016). Properties of latent variable network models. *Network Science* 4, 407–432.
- Rietveld, P. and P. Wintershoven (1998). Border effects and spatial autocorrelation in the supply of network infrastructure. *Papers in Regional Science* 77(3), 265–276.
- Robins, G., P. Pattison, and P. Elliott (2001). Network models for social influence processes. *Psychometrika* 66, 161–189.
- Robins, G., T. Snijders, P. Wang, M. Handcock, and P. Pattison (2007). Recent developments in exponential random graph ( $p^*$ ) models for social networks. *Social Networks* 29(2), 192–215. Special Section: Advances in Exponential Random Graph ( $p^*$ ) Models.
- Salter-Townshend, M. and T. H. McCormick (2017). Latent space models for multiview network data. *The Annals of Applied Statistics* 11(3), 1217 – 1244.
- Scott, D., I. Dam, and R. Wilton (2012). Investigating the effects of social influence on the choice to telework. *Environment and Planning A* 44.

- Sewell, D. K. and Y. Chen (2015). Latent space models for dynamic networks. *Journal of the American Statistical Association* 110, 1646–1657.
- Sewell, D. K. and Y. Chen (2017). Latent Space Approaches to Community Detection in Dynamic Networks. *Bayesian Analysis* 12(2), 351–377.
- Shakarian, P., A. Bhatnagar, A. Aleali, E. Shaabani, and R. Guo (2015). *The Independent Cascade and Linear Threshold Models*, pp. 35–48. Cham: Springer International Publishing.
- Sijtsema, J. J., T. Ojanen, R. Veenstra, S. Lindenberg, P. H. Hawley, and T. D. Little (2010). Forms and functions of aggression in adolescent friendship selection and influence: A longitudinal social network analysis. *Social Development* 19(3), 515–534.
- Simpkins, S. D., D. R. Schaefer, C. D. Price, and A. E. Vest (2013). Adolescent friendships, bmi, and physical activity: Untangling selection and influence through longitudinal social network analysis. *Journal of Research on Adolescence* 23(3), 537–549.
- Sun, J. and J. Tang (2011). A survey of models and algorithms for social influence analysis. In C. C. Aggarwal (Ed.), *Social Network Data Analytics*, pp. 177–214. Boston, MA: Springer US.
- Sweet, T. and S. Adhikari (2020). A latent space network model for social influence. *Psychometrika* 85, 251–274.
- Urberg, K. A., S. M. Değirmencioğlu, and C. Pilgrim (1997). Close friend and group influence on adolescent cigarette smoking and alcohol use. *Developmental psychology* 33(5), 834 –844.
- Vitale, M. P., G. C. Porzio, and P. Doreian (2016). Examining the effect of social influence on student performance through network autocorrelation models. *Journal of Applied Statistics* 43(1), 115–127.
- Wang, S. S., S. Paul, and P. De Boeck (2019). Joint latent space model for social networks with multivariate attributes. *Available at [arxiv.org/abs/1910.12128](https://arxiv.org/abs/1910.12128)*.
- Zheng, K., R. Padman, D. Krackhardt, M. P. Johnson, and H. S. Diamond (2010). Social networks and physician adoption of electronic health records: insights from an empirical study. *Journal of the American Medical Informatics Association* 17(3), 328–336.